Repetition enhancement of amygdala and visual cortex functional connectivity reflects nonconscious memory for negative visual stimuli

Sarah M. Kark[1],*, **Scott D. Slotnick**[1], and **Elizabeth A. Kensinger**[1]

[1]Department of Psychology, McGuinn Hall Room 300, Boston College, 140 Commonwealth Avenue, Chestnut Hill, MA, USA 02467

Abstract

Most studies using a recognition memory paradigm examine the neural processes that support the ability to consciously recognize past events. However, there can also be nonconscious influences from the prior study episode that reflect repetition suppression effects—a reduction in the magnitude of activity for repeated presentations of stimuli—that are revealed by comparing neural activity associated with forgotten items to correctly rejected novel items. The present fMRI study examined the effect of emotional valence (positive vs. negative) on repetition suppression effects. Using a standard recognition memory task, 24 participants viewed line drawings of previously studied negative, positive, and neutral photos intermixed with novel line drawings. For each item, participants made an old–new recognition judgment and a sure–unsure confidence rating. Collapsed across valence, repetition suppression effects were found in ventral occipital-temporal cortex and frontal regions. Activity levels in the majority of these regions were not modulated by valence. However, repetition enhancement of the amygdala and ventral occipital-temporal cortex functional connectivity reflected nonconscious memory for negative items. In this study, valence had little effect on activation patterns but had a larger effect on functional connectivity patterns that were markers of nonconscious memory. Beyond memory and emotion, these findings are relevant to other cognitive and social neuroscientists that utilize fMRI repetition effects to investigate perception, attention, social cognition, and other forms of learning and memory.

INTRODUCTION

Although most studies using recognition memory paradigms examine the neural processes that support the ability to consciously retrieve past events, there can also be implicit (or "nonconscious") influences from prior study episodes, as evidenced by repetition suppression effects (Grill-Spector, Henson, & Martin, 2006; Schott et al., 2006; Logan, 1990). Repetition suppression, a reduction in BOLD fMRI over repeated presentations of familiar visual stimuli, is thought to reflect sharpening (fewer neurons/sparser representation of a stimuli), facilitation (less processing time), or neuronal fatigue (less activation; for

*Please address correspondence to: Sarah M. Kark, kark@bc.edu, 617-552-6949, Department of Psychology, Boston College, McGuinn Hall Room 300, 140 Commonwealth Avenue, Chestnut Hill, MA, USA 02467.
Reprint requests should be sent to Sarah M. Kark, Department of Psychology, Boston College, McGuinn Hall Room 300, 140 Commonwealth Avenue, Chestnut Hill, MA 02467, or via kark@bc.edu.

theoretical reviews of repetition suppression, see Henson, 2015; Grill-Spector et al., 2006). Across paradigms, repetition suppression effects are typically reported in regions of ventral occipitotemporal cortex (for visual stimuli) and the PFC (Vidyasagar, Stancak, & Parkes, 2010; Race, Shanker, & Wagner, 2009; Grill-Spector et al., 2006; Henson, 2003; Buckner et al., 1998; Schacter & Buckner, 1998). These changes in visual processing regions are thought to reflect nonconscious memory for visual stimuli (Vidal et al., 2014; Tulving & Schacter, 1990).

Although repetition effects are often examined by using paradigms in which participants are not consciously aware that an item was previously presented, repetition effects also can be revealed in traditional recognition memory paradigms by comparing correctly rejected new items (first exposure) to forgotten old items (second exposure; Danckert, Gati, Menon, & Kohler, 2007; Slotnick & Schacter, 2006; Henson, Hornberger, & Rugg, 2005; Henson, Cansino, Herron, Robb, & Rugg, 2003; Rugg et al., 1998). In both of these cases, the subjective response from the participant is that the stimuli are "New," but the study history is different. Although repetition suppression effects have been leveraged to demonstrate non-conscious memory for forgotten items (compared with correct rejection of lures) in traditional memory paradigms, the effects of valence (negative and positive) on non-conscious memory have yet to be investigated in a standard recognition memory paradigm.

There is mixed evidence for emotional modulation of repetition effects in ventral occipitotemporal cortex and the amygdala. In ventral occipitotemporal cortex, some studies have shown stronger repetition suppression effects for emotional stimuli compared with neutral stimuli (Bradley et al., 2015; Ishai, Pessoa, Bikle, & Ungerleider, 2004; Fischer, Furmark, Wik, & Fredrikson, 2000), whereas others have reported attenuated repetition suppression effects for emotional stimuli compared with neutral stimuli (Rotshtein, Malach, Hadar, Graif, & Hendler, 2001) or, conversely, greater suppression effects for neutral stimuli compared with negative or positive stimuli (Suzuki et al., 2011). In the amygdala, emotional modulation of repetition suppression effects is similarly equivocal to that of the ventral occipitotemporal cortex. Although some studies have reported similar repetition suppression effects in the amygdala for emotional and neutral stimuli (Suzuki et al., 2011; Glascher, Tuscher, Weiller, & Buchel, 2004; Fischer et al., 2000, 2003; Wright et al., 2001), others report greater repetition suppression effects in the amygdala to repeated negative stimuli compared with neutral stimuli (Bradley et al., 2015; Yang, Cao, Xu, & Chen, 2012; Strauss et al., 2005; Ishai et al., 2004; Phan, Liberzon, Welsh, Britton, & Taylor, 2003; Breiter et al., 1996). The heterogeneity of findings is likely due to some combination of task effects (e.g., number of repetitions or concurrent cognitive tasks), stimuli (e.g., familiar or unfamiliar), or power issues. Furthermore, few studies have included positive stimuli alongside negative and neutral stimuli. However, one such study found a lack of repetition suppression for repeated happy faces compared with neutral faces in ventral occipitotemporal cortex (Suzuki et al., 2011). In the current study, we examined nonconscious memory for forgotten negative, positive, and neutral familiar visual scenes that were consciously encoded.

There is evidence from explicit emotional memory studies to expect that valence will influence nonconscious signatures of memory in the amygdala and the ventral occipitotemporal cortex. First, the key role of the amygdala in implicit and explicit

emotional memory is well established (for reviews, see Murty, Ritchey, Adcock, & LaBar, 2011; Phelps & LeDoux, 2005). Second, there is consistent evidence in the literature that activity in ventral occipitotemporal cortex regions supports encoding (Mickley & Kensinger, 2008; Kensinger, Garoff-Eaton, & Schacter, 2007) and retrieval (Keightley, Chiew, Anderson, & Grady, 2011; Kensinger & Schacter, 2007) of negative visual stimuli to a greater degree than positive and neutral visual stimuli. Furthermore, previous work has shown that retrieval-related recapitulation of ventral occipitotemporal cortex activity engaged during successful encoding supports later recognition of negative visual scenes— but not positive or neutral scenes—and this recapitulation is guided by enhanced amygdala and ventral occipitotemporal cortex coupling during successful encoding (Kark & Kensinger, 2015). Thus, it is possible that activity and functional connectivity of these regions can provide signatures of nonconscious memory, even in the absence of conscious recovery.

We were also interested in examining emotion modulation of repetition effects in medial prefrontal regions. The dorsomedial PFC (dmPFC) has been associated with increased activation during explicit elaboration of negative emotional memories compared with positive emotional memories (Ford, Morris, & Kensinger, 2014) and also more rapid habituation to fearful stimuli compared with neutral stimuli (Wendt, Schmidt, Lotze, & Hamm, 2012). The ventromedial PFC (vmPFC) is involved in emotion processing (Winecoff et al., 2013), but repetition effects in this region might not be modulated by emotion (Bradley et al., 2015). Because both dmPFC and vmPFC have been implicated in emotion evaluation (Dolcos, LaBar, & Cabeza, 2004), we anticipated stronger repetition effects in medial PFC regions for emotional stimuli compared with neutral stimuli.

Recent work has also examined nonconscious memory effects revealed by repetition enhancement effects (Recasens, Leung, Grimm, Nowak, & Escera, 2015; Vannini, Hedden, Sullivan, & Sperling, 2013). Emerging evidence suggests that nonconscious memory effects might be related to repetition-related enhancement (increases) in functional connectivity between task-relevant regions (i.e., increased neural synchrony; for a review, see Segaert, Weber, de Lange, Petersson, & Hagoort, 2013). These studies offer a new approach to assessing nonconscious memory signatures that might go undetected when only repetition suppression of activity is assessed. In the present fMRI study, we asked the question: Are there valence-specific non-conscious memory signatures reflected in repetition-enhanced functional connectivity of the amygdala and visual cortex?

The amygdala and visual cortex are anatomically and functionally positioned to exhibit changes in functional connectivity related to nonconscious memory in the context of a standard recognition paradigm. First, the anatomical connectivity (Amaral, Behniea, & Kelly, 2003) and functional connectivity (Mickley Steinmetz, Addis, & Kensinger, 2010; Robinson, Laird, Glahn, Lovallo, & Fox, 2010; Vuilleumier, Richardson, Armony, Driver, & Dolan, 2004) between the amygdala and the visual cortex are well established. Furthermore, it has been suggested that feedback projections from the amygdala to category-specific sensory processing regions might reflect prior exposure to a particular stimulus during nonconscious memory (Thomas & LaBar, 2005; Breiter et al., 1996). In regards to valence-specific effects, explicit memory studies have shown that increased amygdala and visual

cortex connectivity supports subsequent memory of negative stimuli (Kark & Kensinger, 2015; Mickley Steinmetz et al., 2010), whereas successful encoding of positive stimuli has been associated with decreased connectivity between these regions (Mickley Steinmetz et al., 2010). We hypothesized a valence-specific nonconscious memory signature for negative stimuli evident in repetition enhancement of amygdala and ventral occipital-temporal cortex connectivity.

The current study used a traditional recognition memory paradigm to examine the effects of valence on two types of nonconscious memory signatures: We examined the effect of valence on repetition suppression-related changes in the magnitude of activity and repetition enhancement-related changes in functional connectivity of the amygdala. Participants completed a recognition memory task in which they were shown line drawings of negative, positive, and neutral photos that they had previously studied and an equal number of line drawings of photos they had not seen before. For each item, participants made an old–new recognition judgment and a sure–unsure confidence judgment. We implemented a parametric modulation approach that allowed us to examine implicit memory strength and repetition effects for forgotten items as a function of valence. The novel use of line drawings allowed for three advantages: (1) the ability to cue specific memories without re-presenting the full color images seen at encoding, (2) the use of retrieval cues with less emotional valence and arousal than the original images, and (3) the creation of a challenging recognition task that yielded a sufficient number of correct rejections and forgotten items for analysis.

Broadly, these results provide evidence for the hypothesis that repetition enhancement of functional connectivity can reflect differences in cognitive processing (Segaert et al., 2013). Many different subdisciplines in the fields of cognitive and social neuroscience have utilized repetition suppression effects to study perception (Thurman, van Boxtel, Monti, & Lu, 2015), attention (Schmitz, Dixon, Anderson, & De Rosa, 2014), social cognition (Jenkins, Macrae, & Mitchell, 2008), as well as other forms of learning and memory. Additionally, repetition suppression effects have been used to investigate healthy aging (Schmitz et al., 2014) and clinical populations (e.g., autism [Ewbank et al., 2015], Alzheimer's [Pihlajamaki, O'Keefe, O'Brien, Blacker, & Sperling, 2011]). However, very few studies have leveraged repetition enhancement of activity—much less enhanced functional connectivity—to examine their research questions (Segaert et al., 2013). Hence, in addition to the clear relevance for those investigating nonconscious memory and emotion, repetition-enhanced functional connectivity offers an alternative analysis approach for basic science and clinical researchers.

METHODS

Participants

Twenty-eight participants were recruited from Boston College and the greater Boston area and met eligibility criteria for the study. One participant was dismissed and not scanned due to endorsement of depressive symptoms, and three scanned participants were excluded from the analysis: two participants due to excessive movement in the scanner and one participant due to a technical failure resulting in loss of behavioral data. This resulted in 24 participants (12 women) aged 19–35 years ($M = 23.13$; standard deviation [SD] = 3.72).[1]

Participants were healthy, right-handed, young adult native English speakers, with normal or corrected-to-normal vision. Participants reported no history of head injury, learning disorders, neurological or psychiatric problems, or medications affecting the CNS. Participants were screened for MRI environment contradictions before entering the scanner. The Boston College institutional review board approved this study, and written informed consent of study procedures was obtained from all participants. Participants were compensated $25/hr for their participation.

Stimuli

Stimuli were 300 International Affective Picture System (IAPS) images (100 negative, 100 positive, and 100 neutral). Negative and positive images were prematched on arousal (negative items: $M = 5.54$, $SD = 0.62$; positive items: $M = 5.43$, $SD = 0.61$) and absolute valence (negative items: $M = 2.04$, $SD = 0.79$; positive items: $M = 2.07$, $SD = 0.58$) using the IAPS normative database. Two-tailed independent sample t tests confirmed that negative images were more valenced ($t(198) = 19.28$, $p < .001$) and arousing ($t(198) = 23.14$, $p < .001$) than neutral images (arousal: $M = 3.28$, $SD = 0.76$; absolute valence: $M = 0.42$, $SD = 0.31$). Positive images were also more emotional ($t(198) = 25.01$, $p < .001$) and arousing ($t(198) = 22.17$, $p < .001$) than neutral images. The line drawings of the IAPS images were generated using an in-house MATLAB (The MathWorks, Natick, MA) script and Adobe (San Jose, CA) Photoshop (see Figure 1 for depictions of stimuli).

Procedures

During encoding, participants viewed line drawings of IAPS photos that had negative, positive, or neutral valence followed by the complete color image (i.e., they viewed each line drawing outline for 1.5 sec immediately followed by the complete image for 2 sec; see Figure 1 for sample images and their corresponding line drawings). Participants were presented with 150 of these image sets (50 negative, 50 positive, 50 neutral). To ensure participants were actively encoding the images, participants were asked to indicate whether they would "Approach the scene" or "Back away from the scene" for each complete image.

After a 20-min delay, participants were given a surprise recognition memory test while still in the scanner. All participants were shown 300 line drawings during the recognition task: 150 previously studied photos (i.e., a second exposure) and 150 new line drawings of photos (negative, positive, and neutral) they never studied (i.e., a first exposure). Each line-drawing was presented for 3 sec (see Figure 1). For each item, participants were asked to make an old–new recognition judgment and a sure–unsure confidence rating using the following scale: 1 = *sure the corresponding photo was not studied*, 2 = *unsure, but think the corresponding photo was not studied*, 3 = *unsure, but think the corresponding photo was studied*, 4 = *sure the corresponding photo was studied* (see Figure 1). All responses were

---

[1]The number of participants in this study is larger than the number of participants ($n = 17$) in the original study (Kark & Kensinger, 2015). Since the original study, four additional participants were scanned ($n = 28$ total). Two of the new participants had excessive movement in the scanner and were excluded from these analyses. One of the original participants had a technical problem (Kark & Kensinger, 2015) that resulted in the loss of behavioral data and again could not be analyzed. In the current study, we used a parametric approach, and therefore, we did not need to exclude participants based on the number of trials per condition. Hence, there is a discrepancy in sample size between these two studies.

made using a handheld MRI-safe button box. During the encoding and retrieval task, a fixation cross was displayed between trials for 0.5–9.5 sec to introduce random jitter.

Two study lists were used to vary which half of the items each participant had studied. Because of a programming error, one neutral photo was repeated and therefore removed from all analyses. Stimuli were presented on a MacBook (Apple Computer, Cupertino, CA) using MacStim (White Ant Publishing, Melbourne, Australia). Stimuli in the scanner were viewed using a rear projection system viewed through a mirror mounted to the head coil.

After the recognition task, participants were removed from the scanner and shown the IAPS images used in the study phase and were asked to rate each image's arousal and valence on a 1–7 scale. After the postscan ratings were collected, participants were debriefed, compensated for their participation, and dismissed.

fMRI Data Acquisition and Preprocessing

Structural and functional images were acquired on a Siemens Tim Trio 3-T scanner (Siemens Erlangen, Germany) equipped with a 32-channel head coil. A functional localizer and autoalign scout were followed by collection of whole-brain T_1-weighted anatomical images (MPRAGE, 176 sagittal slices, 1.0 mm^3 voxels, TR = 2530 msec, TE1 = 1.64 msec, TE2 = 3.5 msec, TE3 = 5.36 msec, TE4 = 7.22 msec, flip angle = 7°, 256 field of view, base resolution = 256) and T_2-weighted echo-planar images were acquired in an interleaved fashion, with the slices oriented perpendicular to the long axis of the hippocampus (47 slices, 3.0 mm^3 voxels, TR = 3000 msec, TE = 30 msec, flip angle = 85°, 216 field of view, base resolution = 72). A total of four functional runs were collected during the recognition phase. A distortion-unwarping protocol was employed to correct for asymmetric distortions inherent in coronal slice acquisition. This method implemented a pixel-by-pixel displacement map, derived from a pair of alternately phase encoded spin-echo EPI images acquired before the first BOLD scan, to correct each time point of the subsequent BOLD series as they were reconstructed on the scanner (Benner, van der Kouwe, Mainero, Holland, & Dale, 2011; Holland, Kuperman, & Dale, 2010). The first four scans of each run were discarded to allow for equilibrium effects. A diffusion weighted scan and a resting-state scan were collected during the time between encoding and retrieval, but these data will not be discussed here. The results of the subsequent memory (hits vs. misses) encoding data were reported elsewhere (Kark & Kensinger, 2015).

All MRI analyses were carried out using SPM8 (Wellcome Department of Cognitive Neurology, London, United Kingdom) implemented in MATLAB R2014a. All functional images were reoriented, slice time corrected, realigned, coregistered, spatially normalized to the Montreal Neurological Institute (MNI) template (resampled at 3 mm during segmentation and written at 3 mm during normalization), and smoothed using a 6-mm isotropic Gaussian kernel. Artifact Detection Tools (available at www.nitrc.org/projects/artifact_detect) was used to detect motion and global mean intensity outliers during each scan run for each participant. Motion outliers were defined as scans with a translation or rotation exceeding ±3 mm or ±3°, respectively. Global mean intensity outliers were defined as scans with a global mean intensity greater than 3 *SD*s from the mean. Individual scan runs

with more than 10 total outliers were excluded from fMRI analysis. In total, three scan runs were excluded from the analysis.

Parametric Modulation Analysis

Repetition Suppression of Activity: Fixed-effects—We used parametric modulation analysis to examine repetition effects and memory strength. For each participant, high and low confidence Correct Rejections (CRs) and Misses were assigned a condition code as follows: 1 = *high confidence CRs* (HC-CRs), 2 = *low confidence CRs* (LC-CRs), 3 = *low confidence Misses* (LC-Misses), and 4 = *high confidence Misses* (HC-Misses). Repetition suppression effects were identified as regions that showed a negative parametric relation with the condition code, with the highest activity for HC-CRs and the lowest activity for HC-Misses (i.e., HC-CRs > LC-CRs > LC-Misses > HC-Misses). In this way, we could assess linear relationships across all trials that subjectively reported a "New" response but that differed by previous exposure (previously seen or unseen) and confidence.

For each participant, two separate models were run to examine parametric repetition suppression for all items, collapsing across valence (Fixed-effects Model 1), and for each valence modeled separately (Fixed-effects Model 2). RTs varied across trials (see Behavioral Results section), and therefore RTs were entered as an additional parametric regressor. To identify repetition effects above and beyond any effects of RTs, RTs were entered as the first parametric regressor and the condition code as the second parametric regressor. For both models, the last six columns were always the same and contained: all hits modeled independently, all false alarms modeled independently, and four columns to regress out linear drift across four concatenated retrieval runs. Thus, the valence-collapsed model (Model 1) contained nine columns in total: all "New" RT points (CRs and Misses) with their trial-wise RTs and condition codes entered as parametric regressors. The valence-expanded model (Model 2) contained 15 columns total: nine columns that contained negative, positive, and neutral "New" RT points (CRs and Misses) separately, with their trialwise RTs and condition codes entered as parametric regressors for each valence (three columns per valence). For the valence-expanded model, there were averages of 51.42 (SD = 8.1) negative "New" trials, 48.63 (SD = 9.68) positive "New" trials, and 52.08 (SD = 8.4) neutral "New" trials entered into the analysis.

For each participant, eight parametric t images were obtained to examine repetition suppression effects: (1) collapsed across valence (Model 1), (2) for negative "New" items (Model 2), (3) for positive "New" items (Model 2), and (4) for neutral "New" items (Model 2). Contrast analyses were conducted to isolate repetition suppression effects that were stronger for (5) negative "New" items compared with positive "New" items, (6) negative "New" items compared with neutral "New" items, (7) positive "New" items compared with negative "New" items, and (8) positive "New" items compared with neutral "New" items.

Repetition Suppression of Activity: Random-effects—At the group level, the eight fixed-effects parametric t images were entered into 8 one-sample t tests. To examine repetition suppression effects specific to negative and positive valence, we required that a valence category should have both a significant negative parametric relation with the

condition code and a stronger negative parametric relation than the other valence in the comparison. In this way, we were able to use conjunction analyses to isolate regions that showed a significant modulatory effect that was both significantly negative and significantly more negative than the comparison valence (i.e., not driven by a positive parametric relation for the comparison valence).

At the group level, four conjunction analyses were performed: (1) Negative parametric relation for negative items ∩ Negative parametric relationship for negative items stronger than neutral items, (2) Negative parametric relation for negative items ∩ Negative parametric relationship for negative items stronger than positive items, (3) Negative parametric relation for positive items ∩ Negative parametric relationship for positive items stronger than neutral items, and (4) Negative parametric relation for positive items ∩ Negative parametric relationship for positive items stronger than negative items.

Repetition Enhancement of Amygdala Functional Connectivity—We also examined the effect of valence on repetition-enhanced amygdala connectivity. Parametric functional connectivity between the left amygdala and the entire brain during the recognition task was assessed to identify regions exhibiting repetition-enhanced functional connectivity, which was defined as a positive parametric modulation of the condition code. Repetition enhancement of functional connectivity was analyzed for negative, positive, and neutral visual stimuli separately. Parametric functional connectivity analyses were implemented using the generalized psychophysiological interactions (gPPI) toolbox (available at brainmap.wisc.edu/PPI; McLaren, Ries, Xu, & Johnson, 2012).

The left amygdala seed region was built by creating a 6-mm radius sphere around the peak amygdala coordinate identified to have a negative parametric effect in the valence-collapsed model (MNI coordinates x, y, $z = -24, -7, -17$) and masking the 6-mm radius sphere with a 3-D maximum probability mask of the left amygdala (Hammers et al., 2003) to ensure all voxels of the sphere remained in the amygdala (see inset image in Figure 4 for visualization of the left amygdala seed region overlaid on the averaged anatomical).

At the first level and for each participant, the gPPI tool-box was used to (1) create psychological/task regressors, (2) create the physiological variable by estimating the BOLD signal observed in the left amygdala seed region, and (3) calculate the psychophysiological interaction terms by convolving the time course vectors with their corresponding condition code vector. By calculating the interaction terms, we were able to estimate functional connectivity across the entire brain with the amygdala seed region as a function of condition code. That is, we examined the regions that showed a positive parametric effect of the condition code that reflected an increase in amygdala connectivity from HC-CRs to HC-Misses.

At the first level, three parametric connectivity t images were created for each participant (one for each valence category compared with baseline). The contrast images were entered into three separate one-sample t tests at the group level. At the group level, this model was used to assess regions in which left amygdala connectivity was enhanced linearly across the condition code levels.

Follow-up Approach in ROIs—We were specifically interested in repetition effects in regions of the ventral occipital-temporal cortex, the medial PFC, and the amygdala. Follow-up analyses queried for effects of valence in ROIs that showed repetition suppression effects in the valence collapsed parametric approach by extracting estimates of the slope of the linear relationships for each participant from Fixed-effects Model 2 (see Repetition Suppression of Activity: Fixed Effects section for a description of Model 2 and Valence-collapsed Repetition Suppression Effects section for results). We also extracted slopes from each participant's gPPI beta image (one for each valence) to compare the slope of the repetition enhancement effects of functional connectivity across valences (see Repetition Enhanced Amygdala Functional Connectivity section).

Unless otherwise specified, ROIs (5-mm radius spheres) were built using the MarsBar toolbox (marsbar.sourceforge.net/) and used to extract signal intensity magnitudes (beta values) by condition using the REX toolbox (web.mit.edu/swg/software.htm). Unless otherwise specified, extracted data were analyzed using paired two-sample *t* tests.

Thresholding and Visualization—Unless otherwise specified, an individual voxel threshold of $p < .005$ was used with a 17-voxel extent. This combination was determined to correct for multiple comparisons at $p < .05$, using Monte Carlo simulations (https://www2.bc.edu/sd-slotnick/scripts.htm). Although we focus our discussion on clusters that reach this corrected threshold, we report all clusters with at least 10 contiguous voxels in the tables to avoid Type II error (see Lieberman & Cunningham, 2009, for a discussion). Unless otherwise specified, all visualizations of activation shown in the figures reflect a 17-voxel extent threshold. All MNI coordinates from SPM8 were converted to Talaraich coordinates using the GingerAle tool (Lancaster et al., 2007). For clusters larger than 300 voxels, the coordinate at the center of mass is reported in the tables. Visualizations were created in MRI-croGL (www.mccauslandcenter.sc.edu/mricrogl/). Data were overlaid on the average anatomical brain of the 24 participants (see inset images in Figure 2 and Figure 4), which were created using the imcalc feature in SPM8.

RESULTS

Behavioral Results

Memory performance (d') was high for negative ($M = 1.36$, $SE = 0.1$), positive ($M = 1.48$, $SE = 0.13$), and neutral ($M = 1.27$, $SE = 0.08$) stimuli. Two-tailed paired sample *t* tests showed that memory performance for positive stimuli was greater than for neutral stimuli ($t(23) = 2.45$, $p = .022$), but memory performance did not significantly differ between negative and positive stimuli ($t(23) = -1.36$, $p = .187$) or negative and neutral stimuli ($t(23) = 1.05$, $p = .303$).

To evaluate RTs differences across trials, RTs were entered into a 3×2 repeated-measures ANOVA with factors of Valence (negative, positive, neutral) and Response type (CRs, Misses). There was a significant main effect of Valence ($F(2, 46) = 5.11$, $p = .01$), whereby responses to negative and positive trials were slower than to neutral trials, as well as a main effect of Response type ($F(1, 23) = 9.90$, $p = .005$), whereby CR responses were made more quickly than Misses. There was no significant Valence × Response type interaction ($F(2, 46)$

= 2.16, p = .126). Although we did not find behavioral priming effects, they were not anticipated because RTs reflect the time to make an explicit rather than an implicit memory judgment and participants were not asked to make a speeded response. Because RTs varied by valence and by response type, RTs were entered into the parametric model as outlined in Methods (Repetition Suppression of Activity: Fixed-effects section).

The postscan ratings of valence and arousal confirmed that negative images were more arousing ($t(23)$ = 15.17, $p < .001$) and valenced ($t(23)$ = 27.58, $p < .001$) than neutral images. Positive images were also more arousing ($t(23)$ = 8.81, $p < .001$) and valenced ($t(23)$ = 18.97, $p < .001$) than neutral images. Although the IAPS normative database had been used to match negative and positive images on arousal and absolute valence (i.e., distance from neutral valence), the participants in the current study rated negative images as more arousing ($t(23)$ = 9.15, $p < .001$) and higher in absolute valence ($t(23)$ = 6.63, $p < .001$) than positive images. Postscan arousal and valence ratings of IAPS images were not used as covariates in the current fMRI analyses because, at test, participants only viewed line-drawing images created from the full-color IAPS images. Thus, participants either never saw the full IAPS image (for correctly rejected items) or did not explicitly remember it (for missed items).

Valence-collapsed Repetition Suppression Effects

Collapsed across valence, parametric modulation analysis revealed significant repetition suppression effects in bilateral portions of the middle and superior occipital gyri and in large swaths of the ventral occipital-temporal cortex, including the fusiform gyri and the inferior temporal gyri. There were also peak repetition suppression effects in the dorsal and ventral medial PFC, the parietal cortex, and the putamen. Application of the Hammer's bilateral amygdala mask isolated 11 voxels in the left amygdala (MNI coordinates x, y, z = −24, −7, −17) that showed a significant repetition suppression effect within a larger cluster with a peak repetition suppression effect in the putamen (see Figure 2 and Table 1 for all regions). The plots in Figure 2 were created by extracting parameter estimates for CRs and Misses from each participant's individual standard fixed-effects model that modeled CRs and Misses independently.[2]

Next, we queried the repetition suppression effects in the ventral occipital-temporal cortex, the medial frontal regions (dmPFC and vmPFC), and the left amygdala cluster (k = 11) for effects of valence. The majority of regions probed did not show significant effects of valence. The dmPFC (MNI coordinates x, y, z = −9, 59, 37, k = 70) was an exception,[3] showing a significantly larger repetition suppression effect (i.e., a steeper negative slope) for negative items compared with neutral items ($t(23)$ = 2.12, p = .045), with no significant difference between negative and positive items ($t(23)$ = 1.26, p = .22).

---

[2]A standard, valence-collapsed 10-column regression matrix was created for each participant that included: 2 conditions of interest (CRs and Misses collapsed across valence with their trialwise RTs entered as parametric modulators for each condition [4 columns total]), 2 columns to model hits and false alarms independently as nuisance regressors, and 4 columns to regress out linear drift across the four concatenated retrieval runs.

[3]At the cluster level (k = 182), the vmPFC (MNI coordinates x, y, z = −3, 62, −8) showed a significantly steeper negative slope for negative items compared with neutral items ($t(23)$ = 2.24, p = .03) but the slope of negative items was not significantly different from positive items ($t(23)$ = 0.49, p = .63).

Valence-related Repetition Suppression Effects

To directly examine whether there were regions in which valence modulated the strength of the repetition suppression effect, interaction contrasts were used in conjunction with standard parametric contrasts to examine valence-specific repetition suppression effects. There were greater repetition suppression effects for negative items compared with neutral items (Negative parametric relation for negative items ∩ Negative parametric relation for negative items stronger than neutral items) in the right anterior orbital frontal gyrus (OFG; BA 11/47; MNI coordinates x, y, z = 27, 38, −14; k = 29; see Figure 3, activity shown in red). Although the dmPFC showed some stronger repetition suppression effects for negative stimuli compared with neutral stimuli in the ROI analysis in the prior section (Valence-collapsed Repetition Suppression Effects section), the dmPFC was not revealed by the whole-brain analysis. Thus, although repetition suppression effects in the dmPFC showed some evidence of emotional modulation, it was not to a degree that survived significance testing when using the whole-brain analyses. There were no significant effects for negative items greater than positive or vice versa. Furthermore, there were no repetition effects for positive items that were stronger than for neutral items.

Repetition Enhanced Amygdala Functional Connectivity

In addition to examining repetition suppression of activity, we also examined whether there was repetition-enhanced amygdala and ventral occipital-temporal cortex functional connectivity. The functional connectivity analyses revealed repetition enhancement of connectivity between the left amygdala seed region and the occipital cortex for negative items. Specifically, we found increasing left amygdala functional connectivity[4] with bilateral occipital cortex (BA 18/19), including portions of the fusiform gyri[5] and lingual gyri, the left lateral occipital cortex, and regions of the frontal and parietal cortices (see Figure 4, activity shown in green, and Table 2 for all regions). There was no significant repetition enhancement of left amygdala functional connectivity for positive items or neutral items.

Follow-up analyses revealed that for negative items compared with positive items, there was stronger repetition-enhanced functional connectivity of the amygdala and the left inferior occipital gyrus ($t(23)$ = 2.69, p = .013) and the right fusiform gyrus ($t(23)$ = 2.99, p = .007; see bar plots in Figure 4).

To ensure that the repetition enhancement effects of functional connectivity found in these visual processing regions were specific to the amygdala, we ran a control gPPI analysis using a parietal seed region in the post-central gyrus that showed repetition suppression effects (MNI coordinates x, y, z = −39, −31, 49), because we did not anticipate emotional modulation of repetition enhanced functional connectivity between the postcentral gyrus and

---

[4]A similar pattern of functional connectivity with occipital, frontal, and parietal regions was shown when a right amygdala seed region was used (MNI coordinates x, y, z = 24, −7, −17); this right amygdala region showed valence-collapsed repetition suppression effects at a reduced threshold (p < .015). As with the left amygdala, there was no significant repetition enhancement in functional connectivity with this right amygdala region for positive items or neutral items.

[5]A follow-up conjunction analysis of the Repetition Suppression Effects for Negative Items ∩ Repetition Enhancement Effects of amygdala functional connectivity for Negative Items showed a small amount of overlap in bilateral fusiform gyrus (MNI coordinates x, y, z = −33, −73, −14 and MNI coordinates x, y, z = 21, −73, −11). This suggests that, although there might be a small amount of overlap between these signatures of nonconscious memory, they are largely nonoverlapping.

ventral occipitotemporal cortex. The whole-brain functional connectivity results did not reveal any significant enhancement of postcentral gyrus and ventral occipitotemporal cortex connectivity for negative items, only significant repetition enhancement of postcentral gyrus and SMA (MNI coordinates x, y, $z = 9$, −4, 58; $k = 32$) functional connectivity. We also extracted first-level betas (slopes) of repetition enhanced postcentral gyrus functional connectivity from each participant and for each valence condition from the same left inferior occipital gyrus and right fusiform gyrus spheres. One-sample t tests confirmed that there was no significant repetition enhancement of postcentral gyrus functional connectivity with the left inferior occipital gyrus or the right fusiform gyrus region for any of the valence categories ($p > .1$ for all comparisons).

DISCUSSION

The current study had two novel aims: examine the effect of valence on (1) repetition suppression of activity and (2) repetition enhancement of amygdala functional connectivity in a recognition memory paradigm to elucidate the effect of valence on nonconscious memory activity. We demonstrated that parametric modulation analysis could be used to detect common valence-general repetition suppression effects in the ventral occipitotemporal cortex and the PFC in the context of a standard recognition paradigm. This approach permitted us to investigate nonconscious memory effects (repetition suppression and repetition enhanced functional connectivity) as a function of valence.

We did not find convincing emotional modulation of repetition suppression of activity in the amygdala or the ventral occipital-temporal cortex. Whereas some studies have found emotional modulation of repetition suppression effects in the ventral occipital-temporal cortex (Bradley et al., 2015; Yang et al., 2012; Ishai et al., 2004; Fischer et al., 2000) and the amygdala (Yang et al., 2012; Strauss et al., 2005; Ishai et al., 2004; Phan et al., 2003; Breiter et al., 1996), others have reported no significant emotional modulation of repetition suppression effects in the ventral occipital-temporal cortex (Rotshtein et al., 2001) or the amygdala (Suzuki et al., 2011; Glascher et al., 2004; Fischer et al., 2000, 2003; Wright et al., 2001). It is possible that, in the current study, one stimulus repetition (as opposed to multiple exposures in a rapid serial visual presentation paradigm) might not be sufficient to reveal emotion modulatory effects of repetition suppression of activity.

However, during nonconscious memory for negative items, we found new evidence for repetition enhancement of amygdala functional connectivity with large clusters of bilateral occipital cortex, including the lingual and fusiform gyri. Thus, although emotion modulation of repetition suppression effects in the amygdala and visual processing regions did not reach significance, the repetition enhanced functional connectivity results clearly demonstrate a role of visual processing regions in non-conscious memory effects for negative stimuli. With only one repetition during test, changes in functional connectivity might be a more sensitive measure of nonconscious visual memory activity than regional repetition suppression effects. These findings are compatible with the increased neural synchrony theory of repetition enhancement (for a review, see Segaert et al., 2013), which suggests regions involved in stimulus–response mappings might increase their connection via enhanced functional connectivity. These results are also compatible with a prior study that reported a

significant correlation between lateral occipital cortex and amygdala activity over repeated presentations of negative stimuli (Rotshtein et al., 2001), but the authors conducted a within-subject correlation analysis of amygdala and lateral occipital cortex activity and did not use functional connectivity (i.e., psychophysiological interaction effect) methods.

Although enhanced amygdala and visual cortex connectivity has been shown to guide successful explicit encoding processes (Kark & Kensinger, 2015), in the current study enhanced functional connectivity between the amygdala and visual processing regions reflected implicit memory. In agreement with previous work (Thomas & LaBar, 2005; Breiter et al., 1996), feedback projections from the amygdala to occipital regions might reflect prior exposure to a particular stimulus during nonconscious memory, and in this study, these effects might have manifested as enhanced functional connectivity. However, the current data set did not explore directional effects of connectivity. Furthermore, the present nonconscious memory signatures in early visual regions of the visual stream counters previous retrieval-related recapitulation of higher-order visual processing regions, such as the inferior temporal gyrus (BA 20), during explicit recognition of negative visual stimuli (Kark & Kensinger, 2015). Although reactivation of fine-grained representations in early visual regions might not be necessary for explicit retrieval of higher-order sensory representations, such as complex scenes (Bosch, Jehee, Fernandez, & Doeller, 2014), nonconscious memory signatures appear to be reflected in early regions that were likely engaged during initial perception of the stimulus.

The effects of valence on nonconscious memory activity in medial frontal regions were also investigated. When repetition suppression effects from the valence-collapsed analysis were queried for effects of valence, none of the regions showed greater effects for negative stimuli compared with positive stimuli. However, there was evidence for stronger repetition suppression effects for negative stimuli compared with neutral stimuli in the dmPFC. This latter result is compatible with the findings of Wendt and colleagues (2012) that showed greater signal reduction in dmPFC over repeated presentations of fearful stimuli, compared with neutral stimuli. In the whole-brain analysis, the only region that showed valence-related repetition suppression effects of activity was the right anterior OFG, which showed stronger repetition suppression effects for negative items compared with neutral items. Although we did not predict this a priori, the OFG receives information from the ventral visual stream (projections from the anterior inferior temporal gyrus; Romanski, 2012) and has been associated sensory processing of emotional information (Kringelbach & Rolls, 2004). The OFG has shown a stronger relation to subsequent memory for negative visual stimuli than neutral visual stimuli (Kensinger et al., 2007; Kensinger & Schacter, 2006). Our augmented repetition suppression effects for negative items compared with neutral items might reflect nonconscious memory of emotionally negative visual stimulus processing from the prior study episode. However, this is beyond the scope of the current findings and further work is needed to understand the role of the OFG in nonconscious memory for negative visual stimuli.

We have referred to effects of valence (not emotion or arousal more generally) because the effects of repetition suppression and of repetition-enhanced connectivity were quite different for negative and positive items. Unlike negative items, positive items did not show repetition

suppression in the OFG (see Figure 3), and positive and negative items showed very different repetition-related patterns of connectivity with the amygdala (see Figure 4). These differences appear to be incompatible with a general effect of emotion or arousal—which would be expected to lead to similarities in patterns for positive and negative stimuli—and are more consistent with a role for valence. A caveat, however, is that the colorful negative IAPS images were rated by the participants to be more arousing than the colorful positive images; although the reported data are based on an analysis of the line-drawings that were associated with either nonpresented or forgotten IAPS images, it is still possible that these arousal differences exaggerated effects between the negative and positive stimuli. Future research could more thoroughly address the contributions of valence and arousal by sampling positive and negative stimuli of low-, moderate-and high-arousal levels.

Together, our results suggest that both repetition suppression effects of activity and repetition enhancement of functional connectivity can reflect nonconscious memory for previously studied visual stimuli. This study offers evidence for valence-general nonconscious memory signatures in the ventral occipital-temporal cortex and the amygdala in terms of repetition suppression of activity, but valence-specific enhancement of functional connectivity between these regions for negative items. These results suggest nonconscious memory effects in the amygdala associated with valence-specific changes in processing efficiency of forgotten but previously encountered biologically relevant information.

These findings reemphasize the importance of investigating the possibility of repetition suppression and repetition enhancement effects at the level of both regional activity and functional connectivity. The current set of findings also set the stage for a new line of inquiry for the effect stimulus salience more broadly (i.e., reward, self-relevance) on repetition enhancement of connectivity in the study of nonconscious memory. Understanding the effect of emotion on nonconscious memory signatures in healthy individuals has the potential to provide relevant insights for future clinical research that focuses on patients with posttraumatic stress disorder and social anxiety, both of which show altered habituation of the amygdala to emotional stimuli (Sladky et al., 2012; Shin et al., 2005) and implicit memory biases toward negative stimuli (Coles & Heimberg, 2002).

Acknowledgments

References

Amaral DG, Behniea H, Kelly JL. Topographic organization of projections from the amygdala to the visual cortex in the macaque monkey. Neuroscience. 2003; 118:1099–1120. [PubMed: 12732254]

Benner T, van der Kouwe AJ, Mainero C, Holland D, Dale A. Automatic geometric distortion correction for single-shot echo planar imaging. Proceedings of the International Society for Magnetic Resonance in Medicine. 2011; 19:4568.

Bosch SE, Jehee JF, Fernandez G, Doeller CF. Reinstatement of associative memories in early visual cortex is signaled by the hippocampus. Journal of Neuroscience. 2014; 34:7493–7500. [PubMed: 24872554]

Bradley MM, Costa VD, Ferrari V, Codispoti M, Fitzsimmons JR, Lang PJ. Imaging distributed and massed repetitions of natural scenes: Spontaneous retrieval and maintenance. Human Brain Mapping. 2015; 36:1381–1392. [PubMed: 25504854]

Breiter HC, Etcoff NL, Whalen PJ, Kennedy WA, Rauch SL, Buckner RL, et al. Response and habituation of the human amygdala during visual processing of facial expression. Neuron. 1996; 17:875–887. [PubMed: 8938120]

Buckner RL, Goodman J, Burock M, Rotte M, Koutstaal W, Schacter D, et al. Functional-anatomic correlates of object priming in humans revealed by rapid presentation event-related fMRI. Neuron. 1998; 20:285–296. [PubMed: 9491989]

Coles ME, Heimberg RG. Memory biases in the anxiety disorders: Current status. Clinical Psychology Review. 2002; 22:587–627. [PubMed: 12094512]

Danckert SL, Gati JS, Menon RS, Kohler S. Perirhinal and hippocampal contributions to visual recognition memory can be distinguished from those of occipitotemporal structures based on conscious awareness of prior occurrence. Hippocampus. 2007; 17:1081–1092. [PubMed: 17696171]

Dolcos F, LaBar KS, Cabeza R. Dissociable effects of arousal and valence on prefrontal activity indexing emotional evaluation and subsequent memory: An event-related fMRI study. Neuroimage. 2004; 23:64–74. [PubMed: 15325353]

Fischer H, Furmark T, Wik G, Fredrikson M. Brain representation of habituation to repeated complex visual stimulation studied with PET. Neuro Report. 2000; 11:123–126.

Fischer H, Wright CI, Whalen PJ, McInerney SC, Shin LM, Rauch SL. Brain habituation during repeated exposure to fearful and neutral faces: A functional MRI study. Brain Research Bulletin. 2003; 59:387–392. [PubMed: 12507690]

Ford JH, Morris JA, Kensinger EA. Effects of emotion and emotional valence on the neural correlates of episodic memory search and elaboration. Journal of Cognitive Neuroscience. 2014; 26:825–839. [PubMed: 24283491]

Glascher J, Tuscher O, Weiller C, Buchel C. Elevated responses to constant facial emotions in different faces in the human amygdala: An fMRI study of facial identity and expression. BMC Neuroscience. 2004; 5:45. [PubMed: 15548329]

Grill-Spector K, Henson R, Martin A. Repetition and the brain: Neural models of stimulus-specific effects. Trends in Cognitive Sciences. 2006; 10:14–23. [PubMed: 16321563]

Hammers A, Allom R, Koepp MJ, Free SL, Myers R, Lemieux L, et al. Three-dimensional maximum probability atlas of the human brain, with particular reference to the temporal lobe. Human Brain Mapping. 2003; 19:224–247. [PubMed: 12874777]

Henson RN. Neuroimaging studies of priming. Progress in Neurobiology. 2003; 70:53–81. [PubMed: 12927334]

Henson RN. Repetition suppression to faces in the fusiform face area: A personal and dynamic journey. Cortex. 2015; 80:173–174.

Henson RN, Cansino S, Herron JE, Robb WG, Rugg MD. A familiarity signal in human anterior medial temporal cortex? Hippocampus. 2003; 13:301–304. [PubMed: 12699337]

Henson RN, Hornberger M, Rugg MD. Further dissociating the processes involved in recognition memory: An fMRI study. Journal of Cognitive Neuroscience. 2005; 17:1058–1073. [PubMed: 16102237]

Holland D, Kuperman J, Dale A. Efficient correction of inhomogenous static magnetic field-induced distortion in echo planar imaging. Neuroimage. 2010; 50:175–183. [PubMed: 19944768]

Ishai A, Pessoa L, Bikle PC, Ungerleider LG. Repetition suppression of faces is modulated by emotion. Proceedings of the National Academy of Sciences, USA. 2004; 101:9827–9832.

Kark SM, Kensinger EA. Effect of emotional valence on retrieval-related recapitulation of encoding activity in the ventral visual stream. Neuropsychologia. 2015; 78:221–230. [PubMed: 26459096]

Keightley ML, Chiew KS, Anderson JA, Grady CL. Neural correlates of recognition memory for emotional faces and scenes. Social Cognitive and Affective Neuroscience. 2011; 6:24–37. [PubMed: 20194514]

Kensinger EA, Garoff-Eaton RJ, Schacter DL. How negative emotion enhances the visual specificity of a memory. Journal of Cognitive Neuroscience. 2007; 19:1872–1887. [PubMed: 17958489]

Kensinger EA, Schacter DL. Amygdala activity is associated with the successful encoding of item, but not source, information for positive and negative stimuli. Journal of Neuroscience. 2006; 26:2564–2570. [PubMed: 16510734]

Kensinger EA, Schacter DL. Remembering the specific visual details of presented objects: Neuroimaging evidence for effects of emotion. Neuropsychologia. 2007; 45:2951–2962. [PubMed: 17631361]

Kringelbach ML, Rolls ET. The functional neuroanatomy of the human orbitofrontal cortex: Evidence from neuroimaging and neuropsychology. Progress in Neurobiology. 2004; 72:341–372. [PubMed: 15157726]

Lancaster JL, Tordesillas-Gutierrez D, Martinez M, Salinas F, Evans A, Zilles K, et al. Bias between MNI and Talairach coordinates analyzed using the ICBM-152 brain template. Human Brain Mapping. 2007; 28:1194–1205. [PubMed: 17266101]

Lieberman MD, Cunningham WA. Type I and type II error concerns in fMRI research: Re-balancing the scale. Social Cognitive and Affective Neuroscience. 2009; 4:423–428. [PubMed: 20035017]

Logan G. Repetition priming and automaticity: Common underlying mechanisms? Cognitive Psychology. 1990; 22:1–35.

McLaren DG, Ries ML, Xu G, Johnson SC. A generalized form of context-dependent psychophysiological interactions (gPPI): A comparison to standard approaches. Neuroimage. 2012; 61:1277–1286. [PubMed: 22484411]

Mickley Steinmetz KR, Addis DR, Kensinger EA. The effect of arousal on the emotional memory network depends on valence. Neuroimage. 2010; 53:318–324. [PubMed: 20542121]

Murty VP, Ritchey M, Adcock RA, LaBar KS. Reprint of: fMRI studies of successful emotional memory encoding: A quantitative meta-analysis. Neuropsychologia. 2011; 49:695–705. [PubMed: 21414466]

Phan KL, Liberzon I, Welsh RC, Britton JC, Taylor SF. Habituation of rostral anterior cingulate cortex to repeated emotionally salient pictures. Neuropsychopharmacology. 2003; 28:1344–1350. [PubMed: 12784119]

Phelps EA, LeDoux JE. Contributions of the amygdala to emotion processing: From animal models to human behavior. Neuron. 2005; 48:175–187. [PubMed: 16242399]

Pihlajamaki M, O'Keefe K, O'Brien J, Blacker D, Sperling RA. Failure of repetition suppression and memory encoding in aging and Alzheimer's disease. Brain Imaging Behav. 2011; 5:36–44. [PubMed: 21161449]

Race EA, Shanker S, Wagner AD. Neural priming in human frontal cortex: Multiple forms of learning reduce demands on the prefrontal executive system. Journal of Cognitive Neuroscience. 2009; 21:1766–1781. [PubMed: 18823245]

Recasens M, Leung S, Grimm S, Nowak R, Escera C. Repetition suppression and repetition enhancement underlie auditory memory-trace formation in the human brain: An MEG study. Neuroimage. 2015; 108:75–86. [PubMed: 25528656]

Robinson JL, Laird AR, Glahn DC, Lovallo WR, Fox PT. Metaanalytic connectivity modeling: Delineating the functional connectivity of the human amygdala. Human Brain Mapping. 2010; 31:173–184. [PubMed: 19603407]

Romanski, L. Convergence of auditory, visual, and somatosensory information in ventral prefrontal cortex. In: Murray, M., Wallace, M., editors. The neural bases of multisensory processes. Boca Raton, FL: CRC Press/Taylor & Francis; 2012. p. 667-682.

Rotshtein P, Malach R, Hadar U, Graif M, Hendler T. Feeling or features: Different sensitivity to emotion in high-order visual cortex and amygdala. Neuron. 2001; 32:747–757. [PubMed: 11719213]

Rugg MD, Mark RE, Walla P, Schloerscheidt AM, Birch CS, Allan K. Dissociation of the neural correlates of implicit and explicit memory. Nature. 1998; 392:595–598. [PubMed: 9560154]

Schacter DL, Buckner RL. Priming and the brain. Neuron. 1998; 20:185–195. [PubMed: 9491981]

Schott BH, Richardson-Klavehn A, Henson RN, Becker C, Heinze HJ, Duzel E. Neuroanatomical dissociation of encoding processes related to priming and explicit memory. Journal of Neuroscience. 2006; 26:792–800. [PubMed: 16421299]

Segaert K, Weber K, de Lange FP, Petersson KM, Hagoort P. The suppression of repetition enhancement: A review of fMRI studies. Neuropsychologia. 2013; 51:59–66. [PubMed: 23159344]

Shin LM, Wright CI, Cannistraro PA, Wedig MM, McMullin K, Martis B, et al. A functional magnetic resonance imaging study of amygdala and medial prefrontal cortex responses to overtly presented fearful faces in posttraumatic stress disorder. Archives of General Psychiatry. 2005; 62:273–281. [PubMed: 15753240]

Sladky R, Hoflich A, Atanelov J, Kraus C, Baldinger P, Moser E, et al. Increased neural habituation in the amygdala and orbitofrontal cortex in social anxiety disorder revealed by fMRI. PLoS One. 2012; 7:e50050. [PubMed: 23209643]

Slotnick SD, Schacter DL. The nature of memory related activity in early visual areas. Neuropsychologia. 2006; 44:2874–2886. [PubMed: 16901520]

Strauss MM, Makris N, Aharon I, Vangel MG, Goodman J, Kennedy DN, et al. fMRI of sensitization to angry faces. Neuroimage. 2005; 26:389–413. [PubMed: 15907298]

Suzuki A, Goh JO, Hebrank A, Sutton BP, Jenkins L, Flicker BA, et al. Sustained happiness? Lack of repetition suppression in right-ventral visual cortex for happy faces. Social Cognitive and Affective Neuroscience. 2011; 6:434–441. [PubMed: 20584720]

Thomas LA, LaBar KS. Emotional arousal enhances word repetition priming. Cogn Emot. 2005; 19:1027–1047. [PubMed: 26321783]

Tulving E, Schacter DL. Priming and human memory systems. Science. 1990; 247:301–306. [PubMed: 2296719]

Vannini P, Hedden T, Sullivan C, Sperling RA. Differential functional response in the posteromedial cortices and hippocampus to stimulus repetition during successful memory encoding. Human Brain Mapping. 2013; 34:1568–1578. [PubMed: 22344847]

Vidal JR, Perrone-Bertolotti M, Levy J, De Palma L, Minotti L, Kahane P, et al. Neural repetition suppression in ventral occipitotemporal cortex occurs during conscious and unconscious processing of frequent stimuli. Neuroimage. 2014; 95:129–135. [PubMed: 24667455]

Vidyasagar R, Stancak A, Parkes LM. A multimodal brain imaging study of repetition suppression in the human visual cortex. Neuroimage. 2010; 49:1612–1621. [PubMed: 19837182]

Vuilleumier P, Richardson MP, Armony JL, Driver J, Dolan RJ. Distant influences of amygdala lesion on visual cortical activation during emotional face processing. Nature Neuroscience. 2004; 7:1271–1278. [PubMed: 15494727]

Wendt J, Schmidt LE, Lotze M, Hamm AO. Mechanisms of change: Effects of repetitive exposure to feared stimuli on the brain's fear network. Psychophysiology. 2012; 49:1319–1329. [PubMed: 22913381]

Winecoff A, Clithero JA, Carter RM, Bergman SR, Wang L, Huettel SA. Ventromedial prefrontal cortex encodes emotional value. Journal of Neuroscience. 2013; 33:11032–11039. [PubMed: 23825408]

Wright CI, Fischer H, Whalen PJ, McInerney SC, Shin LM, Rauch SL. Differential prefrontal cortex and amygdala habituation to repeatedly presented emotional stimuli. Neuro Report. 2001; 12:379–383.

Yang J, Cao Z, Xu X, Chen G. The amygdala is involved in affective priming effect for fearful faces. Brain and Cognition. 2012; 80:15–22. [PubMed: 22626918]
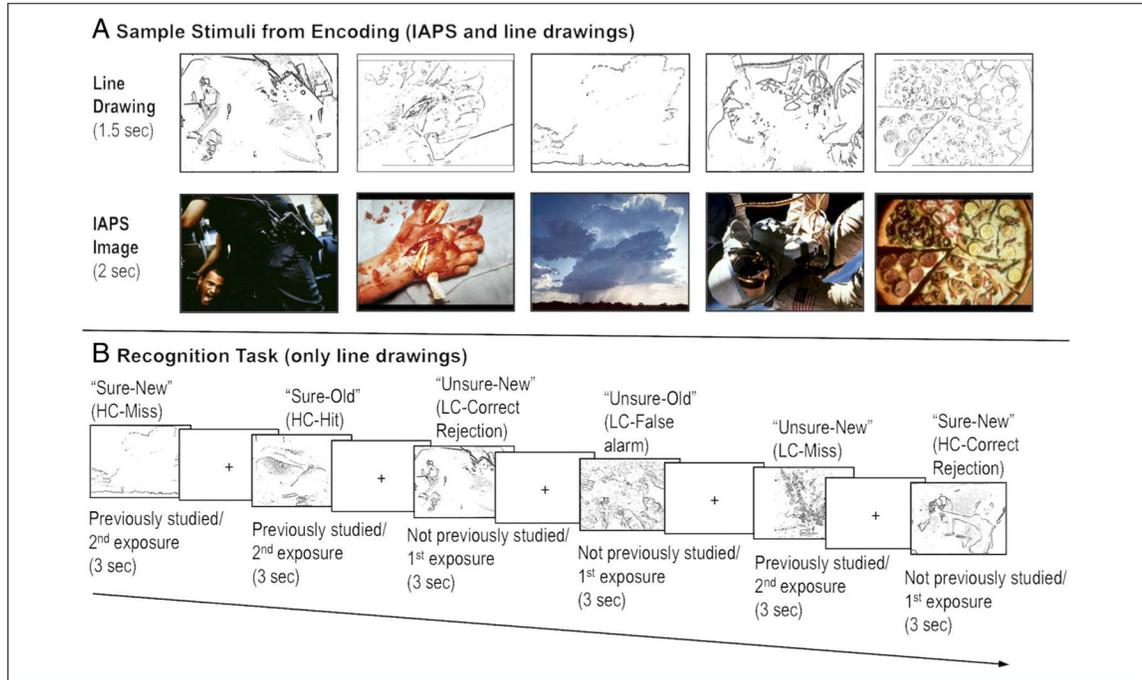
Figure 1.
Sample stimuli and recognition task. (A) Sample negative, positive, and neutral IAPS images with their corresponding line drawings. At encoding, each line drawing was shown for 1.5 sec before the presentation of the IAPS image for 2 sec. (B) Depiction of the recognition task, which involved an old–new judgment and a sure–unsure confidence judgment for each item. Sample response types are listed above each line drawing and are based on whether that line drawing was seen during encoding (a second exposure; i.e., an old line drawing) or if the line drawing had not been seen during encoding (i.e., a first exposure to a lure item).
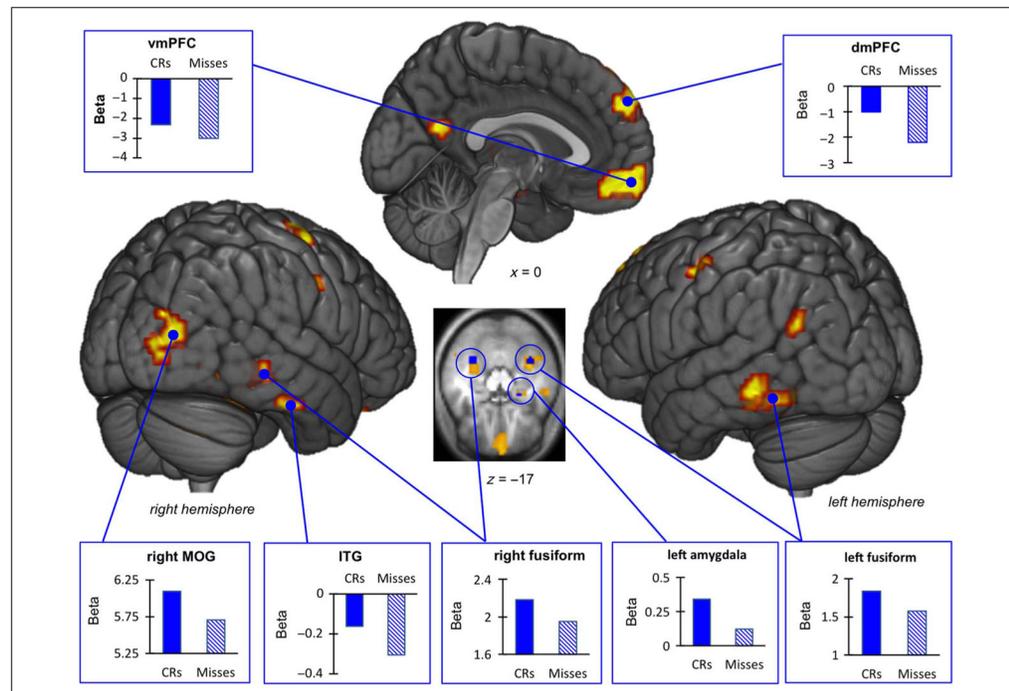
Figure 2.
Valence-collapsed repetition suppression effects. Rendered visualizations of repetition suppression effects as revealed by the parametric approach are shown in yellow. Parameter estimates from the standard general linear model comparing CRs to Misses were extracted from ROIs (visual, medial frontal, and amygdala) and plotted in the blue bar graphs. The inset axial slice shows significant repetition suppression effects in the amygdala and the bilateral fusiform gyri.

Figure 3.
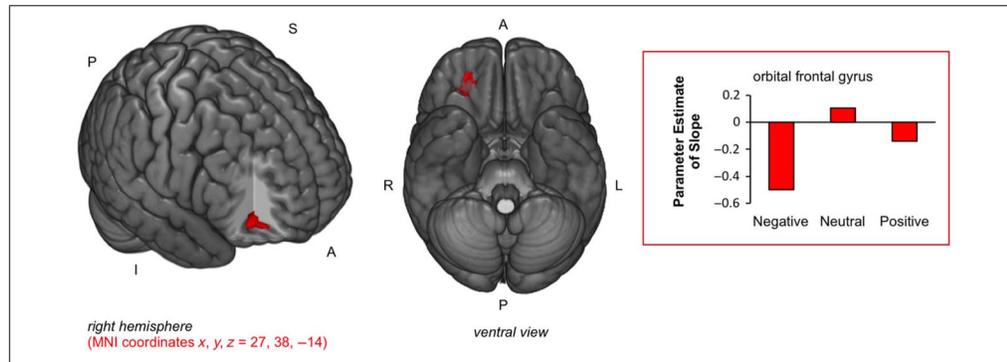Repetition suppression effects for negative items greater than neutral items. There were stronger RS effects (negative slope) in the right OFG for negative items compared with neutral items. Parameter estimates of the parametric analysis slope were extracted from each participant's fixed-effects model (Model 2) and averaged by valence (shown in the bar plot).
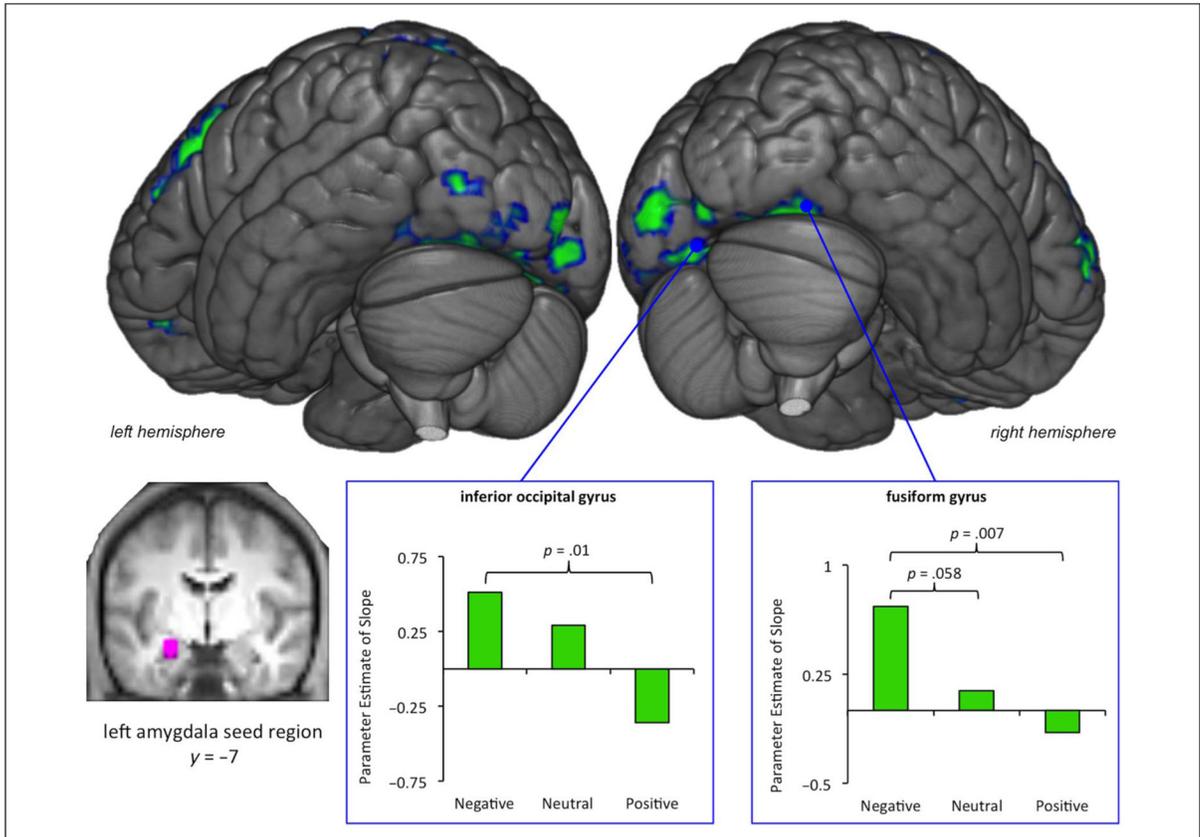
Figure 4.
Repetition enhancement of left amygdala and visual cortex functional connectivity for negative stimuli. Regions that showed a significant positive parametric relationship of condition code (repetition enhancement) are shown in green. The left amygdala seed region (shown in violet) is visualized on a coronal slice of the average anatomic image participants. For the left inferior occipital gyrus (MNI coordinates x, y, $z = -9$, -82, -11) and the right fusiform gyrus (MNI coordinates x, y, $z = 39$, -70, -17), parameter estimates of the slope were extracted from each individual participant's gPPI beta image file (one for each valence) and averaged for each valence (shown in inset green bar graphs).

Table 1

Regions that Showed Valence-collapsed Repetition Suppression Effects (Significant Negative Parametric Relation of Condition Code)

Lobe	Region	Hemisphere	Approximate Brodmann's Area	MNI Coordinates (x,y,z)	Talairach Coordinates (x,y,z)	Voxel Extent (k)
Occipital	Middle occipital gyrus	L	18	−24,−88,−2	−23,−83,−6	35
		R	18	39,−88,13	35,−85,9	74
	Superior occipital gyrus	L	19	−36,−85,34	−35,−84,26	13
		L	19	−30,−70,28	−29,−69,22	76
		R	19	36,−67,37	32,−68,32	17
Temporal	Inferior temporal gyrus,[a] fusiform gyrus,[b] middle temporal gyrus	L	37	−36,−49,−17	−34,−46,−16	339
	Fusiform gyrus,[a,b] inferior temporal gyrus	R	37	33,−49,−17	30,−46,−15	399
	Inferior temporal gyrus	L	20	−45,−7,−26	−42,−6,−20	42
		R	20	63,−34,−26	58,−31,−21	17
	Middle temporal gyrus	R	39	48,−64,25	43,−64,21	14
Frontal	Dorsal medial PFC	L	9	−9,59,37	−10,50,42	70
	Paracentral lobule	L	6	−6,−22,52	−7,−27,48	15
	Precentral gyrus	R	6	39,−10,64	34,−17,61	38
		R	6	54,2,22	49,−2,25	18
	Subcallosal gyrus	R	25	3,8,−17	2,7,−10	16
	Superior frontal gyrus	L	8	−12,44,49	−13,35,52	17
	Ventral medial PFC	L	10	−3,62,−8	−4,57,2	182
Parietal	Postcentral gyrus	L	3	−39,−31,49	−38,−35,44	51
		L	4	−51,−13,55	−49,−18,51	19
		R	2	51,−19,28	46,−22,28	41
		R	3	42,−28,49	37,−32,46	22
		R	1	57,−16,52	51,−21,50	11
	Superior parietal lobule	L	7	−27,−46,73	−27,−51,65	13
Other	Cerebellum	L	N/A	−30,−67,−44	−28,−60,−42	18
		L	N/A	−6,−85,−47	−6,−77,−45	15
		R	N/A	33,−76,−32	30,−70,−31	50
		R	N/A	3,−58,−47	2,−52,−43	14
	Cingulate gyrus	L	31	0,−37,34	−2,−39,31	11

Lobe	Region	Hemisphere	Approximate Brodmann's Area	MNI Coordinates (x,y,z)	Talairach Coordinates (x,y,z)	Voxel Extent (k)
	Precuneus	L	23	−3,−61,19	−4,−60,16	17
	Putamen	L	N/A	−27,−16,10	−26,−17,11	135
		R	N/A	30,−4,7	27,−6,10	11

[a] Signifies the center of mass if $k > 300$.

[b] Signifies the peak region.

Table 2

Regions that Showed Significant Repetition Enhancement of Functional Connectivity with the Left Amygdala Seed Region for Negative Items

Lobe	Region	Hemisphere	Approximate Brodmann's Area	MNI Coordinates (x,y,z)	Talairach Coordinates (x,y,z)	Voxel Extent (k)
Occipital	Fusiform gyrus,[a] lingual gyrus, inferior occipital gyrus, cerebellum[b]	L	18	−9,−82,−11	−9,−77,−13	333
	Fusiform gyrus, cerebellum[b]	R	19	18,−76,−14	16,−71,−15	56
	Fusiform gyrus	R	19	39,−70,−17	35,−66,−17	29
	Lateral occipital cortex	L	19	−48,−82,−2	−46,−78,−6	20
	Lingual gyrus	R	18	9,−94,−11	7,−88,−14	16
Frontal	Middle frontal gyrus[a,b]	R	9/10	45,47,7	41,41,15	351
	Middle frontal gyrus	L	9	−51,11,40	−49,5,40	98
		R	6	42,11,52	37,4,52	10
	Orbital frontal gyrus	L	11	−24,44,−14	−23,41,−5	10
	Precentral gyrus	L	4	−36,−13,61	−35,−19,57	17
	Superior frontal gyrus	L	8	−18,23,61	−18,14,60	15
		L	8	−24,41,46	−24,33,48	14
		R	10	30,65,−5	27,59,6	23
Parietal	Inferior parietal lobule	R	40	51,−31,55	45,−36,51	16
	Precuneus	L	7	−6,−67,40	−7,−68,34	44
	Superior parietal lobule	L	7	−27,−43,67	−27,−48,60	259

[a] Signifies the center of mass if k > 300.

[b] Signifies the peak region.